Electrical conductivity of single-wall carbon nanotube films in strong electric field

D. Seliuta, L. Subačius, I. Kašalynas, M. Shuba, A. Paddubskaya et al.

Citation: J. Appl. Phys. **113**, 183719 (2013); doi: 10.1063/1.4804658
View online: http://dx.doi.org/10.1063/1.4804658
View Table of Contents: http://jap.aip.org/resource/1/JAPIAU/v113/i18
Published by the American Institute of Physics.

Electrical conductivity of single-wall carbon nanotube films in strong electric field

D. Seliuta,[1,2,a)] L. Subačius,[1] I. Kašalynas,[1] M. Shuba,[3] A. Paddubskaya,[3] V. Ksenevich,[4] P. Kuzhir,[3] S. Maksimenko,[3] and G. Valušis[1]
[1]*Optoelectronics Department, Center for Physical Sciences and Technology, A. Goštauto 11, LT-01108 Vilnius, Lithuania*
[2]*Department of Electronic Systems, Vilnius Gediminas Technical University, Naugarduko 41, LT-03227 Vilnius, Lithuania*
[3]*Institute for Nuclear Problems, Belarus State University, Bobruiskaya 11, 220030 Minsk, Belarus*
[4]*Department of Physics, Belarus State University, Nezalezhnastsi Ave. 4, 220030 Minsk, Belarus*

(Received 6 March 2013; accepted 26 April 2013; published online 14 May 2013)

Carrier transport features in single-wall carbon nanotube (SWCNT) films under strong electric fields (up to 10^5 V/cm) are presented. Application of electrical pulses of nanosecond duration allowed to minimize Joule heating and resolve intrinsic nonlinearities with the electric field. Investigations within a wide range of temperatures—4.2–300 K—indicated that carrier localization as well as tunneling through the insulating barriers between conducting regions takes place in SWCNT films. Crossover from semiconducting behavior to metallic behavior in strong electric field is described using the fluctuation induced tunneling model and assuming that the conducting regions demonstrate characteristic metallic conductivity. © *2013 AIP Publishing LLC*. [http://dx.doi.org/10.1063/1.4804658]

I. INTRODUCTION

Although devices based on individual single-wall carbon nanotube (SWCNT) demonstrate excellent physical properties,[1] repeatable production of identical single-tube devices still remains a challenge. Meanwhile, SWCNT aggregates (films, networks, mats) consisting of a large number of SWCNT exhibit uniform physical and electronic properties. Field effect transistors with channels based on SWCNT networks have been demonstrated as a good alternative to single-tube transistors.[2] Thin CNT film is conductive and optically transparent,[3] making it promising for applications as contacts in optoelectronic and photovoltaic devices. In addition, SWCNT films have attracted attention as infrared bolometers,[4,5] strain/stress sensors at the macroscale,[6] gas sensors,[7] and interconnects for large scale integrated circuits.[8]

Properties of SWCNT structures are more complex to interpret with respect to the isolated SWCNT; however, properties of SWCNT structures are interesting both for fundamental and applied physics purposes. Normally, the internanotube junction resistance is much larger than the nanotube resistance itself;[9,10] therefore, understanding of electrical transport properties of SWCNT film requires consideration of intertube contacts. The existing interpretations of the transport properties in SWCNT systems can be classified into two categories: the homogeneously disordered picture with variable range hopping (VRH) mechanism[11,12] and the heterogeneous picture that emphasizes the role of the junctions as energy barriers between metallic regions.[9,13] In real situations, there also may be combinations of the homogeneously disordered part and the heterogeneous conduction part.[12]

Modern electronic devices are continuously being scaled down to nanometer dimensions, leading to high electric field effects induced by moderate bias voltage. Therefore, knowledge of electric-field-dependent properties of SWCNT networks is required for the sake of possible potential applications. Previous investigations of carrier transport in CNT structures have been performed[14–16] only within limits of moderate electric field strength (up to 100–1000 V/cm) in order to avoid Joule heating of CNT layers. On the other hand, isolated SWCNTs were subjected to heating by stronger electric fields.[17,18] Breakdown limit was found to scale linearly with SWCNT length, approximately as 5 V/μm.[18]

In this study, we investigate carrier transport in SWCNT systems in strong electric fields (up to 10^5 V/cm), applying electrical pulses of nanosecond duration allowing hence to minimize the sample heating and resolve time-dependent intrinsic nonlinearities. Investigation within a wide range of temperatures and electric fields has indicated that localization of carriers as well as tunneling through the insulating barriers between conducting regions takes place in SWCNT films. The crossover from semiconductor behavior to metallic behavior in strong electric field is described using the fluctuation induced tunneling model assuming that the conducting regions demonstrate characteristic metallic conductivity.

II. SAMPLE PREPARATION AND MEASUREMENT METHOD

In our investigations, we used purified SWCNT material produced by electric-arc-discharge using nickel-yttrium catalyst (manufacturer CarboLex, Inc.) with SWCNT diameters ranging from 1.2 to 1.5 nm. SWCNTs were stuck in bundles with diameters 3–7 nm and average length 3.5 μm. The suspension of SWCNTs in 1% solution of sodium dodecylsulfate

a)Author to whom correspondence should be addressed. Electronic mail: dalius@pfi.lt

(SDS) in deionised water were prepared by ultrasonication for 4 h (at ultrasonic frequency 44 kHz, intensity 70 W/cm^{-2}) and subsequent centrifugation for 1.5 h at 900 g. Thin SWCNT films of thickness about 100 nm were prepared by spraying the SWCNT suspension (at concentration 0.04 g/l) on hot glass substrate with previously prepared Au contacts. Four parallel Au stripes were lithographically defined enabling the four-contact measurement method. Width of the stripes was 5 μm and separation 5 μm (Fig. 1(a)). The contact stripes are widened on the left-hand side for connection with bonding pads. Electric field was assumed to be uniform and was estimated dividing applied voltage by the distance between the contact stripes.

During spraying process the glass substrates were kept at elevated temperature (100 °C) in order to facilitate evaporation water and partial removal of SDS from the surface of SWCNTs to create better contacts between attached SWCNTs. Later samples were carefully rinsed in deionized water to remove SDS from the SWCNT film.

To decrease the average length some part of SWCNT were ultrasonicated for 3 h in a mixture of concentrated sulfuric and nitric acids (volume fraction 3:1, concentrations 95% and 59%, respectively). To avoid degradation of SWCNT sidewalls, the ultrasonication was conducted at temperature 8 °C.[19] Acid treatment resulted in production of short SWCNTs with average length around 0.5 μm. After the acid treatment, SWCNTs were suspended in SDS water solution and sprayed on the glass plate using previously described method. In the text below, films with original SWCNT are denoted as sample SWCNT-1 and films with acid-treated SWCNT—as sample SWCNT-2.

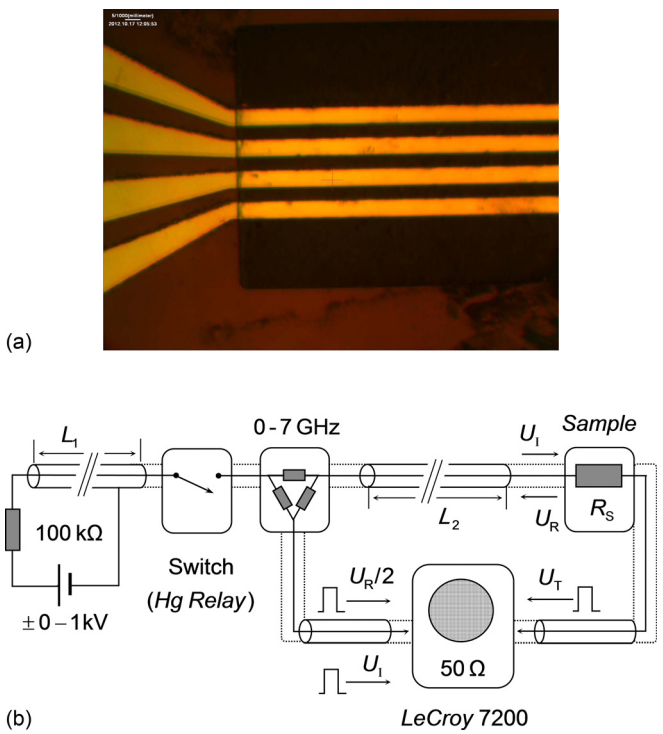

FIG. 1. (a) Photo of the contacts and (b) schematic diagram of the measurement circuit.

Experimentally, to avoid heating of CNT film by electrical power dissipation, nanosecond pulsed characterization technique was applied. Figure 1(b) demonstrates schematic diagram of the measurement circuit using 50 Ω coaxial transmission lines. High-voltage (up to 500 V) rectangular pulses are produced by discharging of coaxial line of length L_1 through the mercury-wetted relay switch, enabling electrical signals with rise and decay times below 0.5 ns. As shown in Fig. 1(b), the charged-line pulse generator is connected to the impedance-matched resistor junction (triangular configuration of three 50 Ω resistors), which allows splitting of the input line into the reference line terminated at the oscilloscope and the output line consisting of the line of length L_2, the sample, and the line connecting the sample with the oscilloscope. Oscilloscope input resistance at both channels is 50 Ω. To avoid overlapping of the incident and the reflected voltage pulses, L_2 is taken greater than L_1.

For analysis of measured oscilloscope traces and to determine current-voltage characteristics of the sample, we used conventional telegrapher's equations. Temporal dependencies of the sample resistance $R_S(t)$, sample current $I(t)$, and sample voltage $U(t)$ are determined from the oscilloscope traces, assuming that dispersion, ohmic, and radiation losses in the coaxial components can be neglected. With experimental conditions, the sample voltage is given as[20]

$$U = U_I + U_R - U_T, \tag{1}$$

where U_I is the incident voltage pulse amplitude, U_R is the reflected pulse amplitude, and U_T is the transmitted pulse amplitude. Sample current is given as[20]

$$I = \frac{U_I - U_R}{Z} = \frac{U_T}{Z}, \tag{2}$$

where Z is the transmission line impedance. Combination of Eqs. (1) and (2) results in $U = 2U_R$. Sample resistance is calculated as $R_S = U/I$.

Current-voltage relation of SWCNT films was measured using voltage pulses of ≈20 ns. Voltage and current pulses are presented in Fig. 2. Sample current and voltage temporal characteristics are presented at three different bias levels.

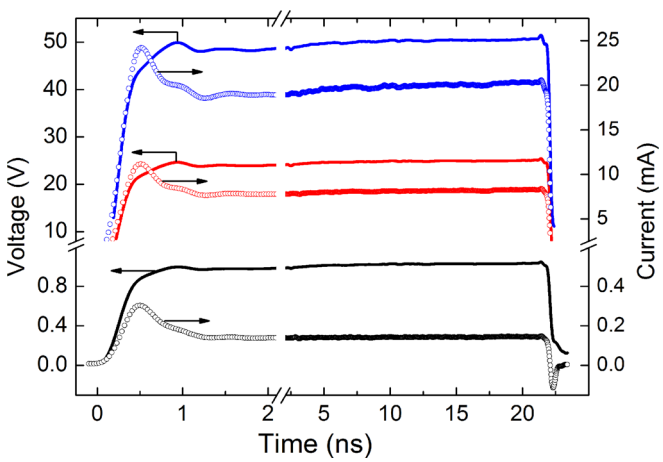

FIG. 2. Time dependence of the sample current (dots) and the sample voltage (lines) at three different pulse amplitudes.

Waveforms show the voltage ringing and transmission-reflection spikes as well as remarkable current overshoot at the rising edge of the pulse due to not perfect matching of the sample to the coaxial transmission line. It is seen in Fig. 2 that current and voltage reach steady values at 1.5 ns independently of applied amplitude. This indicates that temperature of sample remains constant during the pulse. Due to small pulse duration and low repetition rate (55 Hz), overall heating was assumed to be small and was neglected in the following considerations.

Possibility of SWCNT heating during first nanosecond cannot be tested experimentally in our experiment. It was demonstrated that multiwall CNT (MWCNT) films because of their small mass have low heat capacity per unit area and sufficiently fast thermal response for applications in thermophones[21] and display devices.[22] MWCNT films heated to incandescence with 6 ms voltage pulse demonstrate ramp-up and cooling times around 1 ms.[22] It has been reported that standard pulsed current technique in microsecond time scale allows to eliminate sample heating effects from the experimental data[16,23] at moderate electric field strength values in SWCNT films. In this study, we investigate electrical transport in nanosecond time scale what allows us to assume that heating of SWCNT layers can be ignored in our experiments.

Data presented in IV characteristics were taken 10 ns after beginning of each pulse. Normally, two adjacent contacts were used in measurement circuit as shown in Fig. 1. To estimate contribution of electrical contacts between SWCNT film and Au stripes four-wire method was applied using outer contacts for sourcing of current and inner contacts for voltage probing. Comparison of results obtained using the two- and the four-wire methods showed that the contact resistance between SWCNT film and Au stripes can be neglected within the investigated temperature and voltage ranges. The pulsed method was also compared with DC measurements at small voltage values (<1 V) when heating of SWCNT film is negligible. Both methods yielded identical results within 5% systematic error.

III. RESULTS AND ANALYSIS

IV characteristics of sample SWCNT-1 are plotted in Fig. 3 for different temperatures. Detailed analysis shows that IV curves are nonlinear except for small initial part at low voltage values. The linear and nonlinear parts of the conductivity are clearly resolved in Fig. 4 where resistance is plotted as a function of electric field in CNT film at lowest temperature 4 K. Resistance is found to be nonlinear beyond some critical electric field E_c and nearly independent of electric field below E_c. The critical field value E_c is defined as the intersection of the fitting lines to the low field ohmic region (horizontal line) and the high field nonlinear region as demonstrated in Fig. 4. It may be found from Fig. 4 that in nonlinear region resistance decreases with electric field as $E^{-1/3}$. The critical electric field is temperature dependent as shown in the inset of Fig. 4.

Nonlinear resistance with a threshold field indicates possible localization of charge carriers[16] in SWCNT defects,

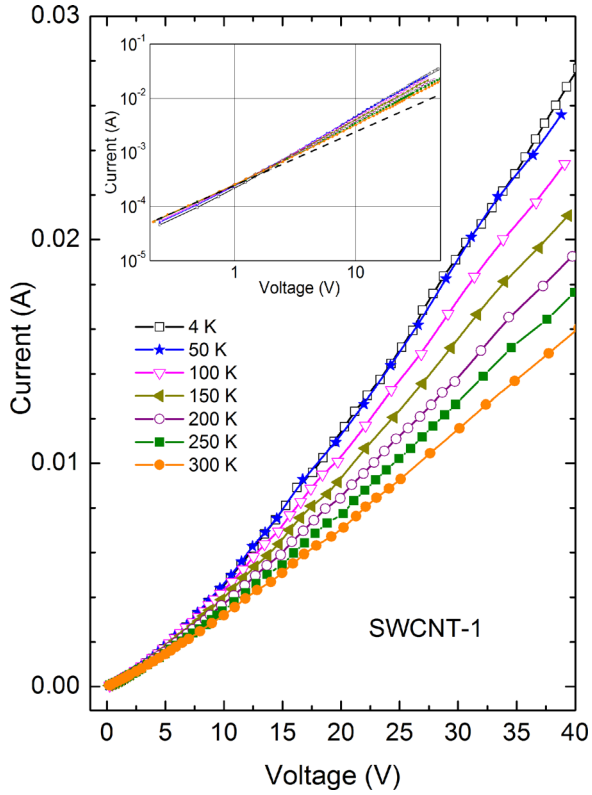

FIG. 3. Current-voltage characteristic of SWCNT film. The connecting lines are given for visual guidance. Inset—initial part of the characteristic in log scale. Dashed line is given for indication of the linear dependence.

intertube contacts, or inter-bundle contacts. Generally, increasing of both the temperature and the electric field strength facilitates release of the localized carriers and contribute to the electrical conductivity of SWCNT layer. If average distance between localization centers is L then energy acquired by a carrier jumping from one localization site to the next is $W_j = eEL$. Ohmic region is set as long as W_j is less than the thermal energy of a carrier kT, while nonlinear region corresponds to $W_j > kT$. Therefore, relation between the critical field E_c and distance L is

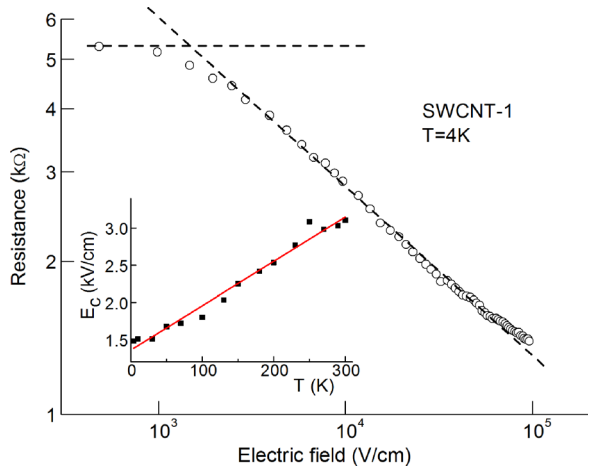

FIG. 4. Resistance of SWCNT layer as a function of electric field strength. Inset—dependence of the critical electric field strength on temperature. Lines are linear fits to data points.

$$E_C = \frac{kT}{eL}. \quad (3)$$

In our case, the critical field is a linear function of temperature; however, the critical field does not follow exactly Eq. (3) at low temperature limit approaching some constant value around 1360 V/cm (see inset in Fig. 4). It implies that localization of carriers possibly takes place in SWCNT films; however, additional conduction mechanisms must be taken into account to find better approximation of the experimental results.

To further characterize the electronic transport properties and the mechanism of conduction in SWCNT layers, we analyze the temperature dependence of the resistance of SWCNT films at various electric field strength values (Fig. 5). It is seen that at electric field 3 kV/cm resistance is almost independent of temperature. It means that there is a crossover electric field E^* roughly at 3 kV/cm so that below E^* (weak electric fields) dR/dT is negative (semiconductor behavior) and above E^* (strong electric fields) dR/dT is positive (metallic behavior). The crossover electric field E^* approximately corresponds to the critical electric field E_C at 300 K (see inset in Fig. 4).

To our knowledge, the transition from semiconducting behavior to metallic behavior in SWCNT films with increasing electric field has not been reported before. It seems natural as in previous publications electrical transport in SWCNT structures was investigated only in moderate electric fields (not exceeding 100–1000 V/cm). To explain the strong electric field data, we will apply commonly used carrier transport mechanisms in SWCNT structures.

Two basic models have been proposed and widely used to describe electrical conductivity of SWCNT networks: homogeneous model based on charge carrier localization and hopping between localization sites[11,12,24] and heterogeneous (called fluctuation induced (assisted) tunneling or FIT)[9,13,24] model. In the latter model, it is assumed that most of carriers are delocalized and move freely over conducting regions very large compared with atomic dimensions. For these random systems, the electrical conductivity is dominated by tunneling of carriers across the insulating gaps between the conducting regions. Because dimensions of the tunneling gaps are small, thermally activated voltage fluctuations across the barriers introduce temperature dependence of the tunneling probability. In SWCNT networks, potential barriers are considered to originate from intertube or interbundle contacts. Localization of carriers near defects is also a possible cause of the barriers to conduction.[9]

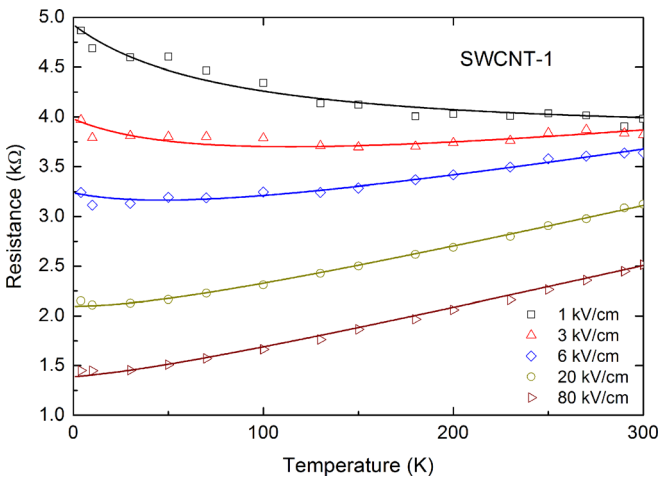

FIG. 5. Dependence of the resistance of SWCNT layers on temperature at different electric field values. Lines are fits to Eq. (4).

As it was discussed, VRH model based on localization of carriers is not completely consistent with our results. Moreover, VRH model cannot account for positive dR/dT (metallic behaviour of SWCNT film) at high electric field since phonons facilitate electron hopping process and, consequently, resistance always decreases with increase of temperature. At strong electric fields contribution of phonons becomes relatively small; therefore, resistance becomes independent of temperature.[25]

Alternatively, the mixed metallic-nonmetallic character of the conductivity of SWCNT films has been attributed to series conduction of conducting islands that is interrupted by small tunneling barriers. In case when the conducting islands have linear metallic resistivity, the resistivity of SWCNT film may be given as[9]

$$R(T) = AT + Be^{\frac{T_C}{T+T_S}}, \quad (4)$$

where the first term accounts for the quasi-1-D metallic conduction in metallic SWCNT, and the second term corresponds to FIT between metallic SWCNT regions, A and B are geometrical factors depending on distribution of the conducting and insulating regions across the sample, T_C and T_S are constants.

FIT model is consistent with the positive dR/dT observed in strong electric fields. Factor A in Eq. (4) is positive as conductivity in metallic SWCNT is dominated by backscattering of electrons due to emission of phonons; therefore, resistance of metallic SWCNT increases with temperature.[26] Semiconducting SWCNTs that are normally present in nonsorted SWCNT structures are normally ignored, assuming that conductivity of semiconducting SWCNT is much less than that of metallic SWCNT. Therefore, contribution of semiconducting SWCNT to the conducting SWCNT network was not taken into account.

We show in Fig. 5 that Eq. (4), which includes the metallic term and FIT term, gives a good account of the experimental R-T characteristics. Solid lines are plotted using Eq. (4) and fitting parameters presented in Table I.

Equation (4) has been used in weak and moderate electric fields (up to 100–1000 V/cm) to account for crossover from semiconducting conductivity at lower temperatures to metallic conductivity at higher temperatures. For investigated sample, we have found that the crossover occurs with increasing electric field strength.

According to Sheng's model,[13] electric field modifies the potential barriers between the conductive regions in such a way that effective barrier width and height are reduced and, consequently, sample resistance decreases. It follows that at sufficiently high electric field the barrier contribution to the sample resistance becomes small compared to the

TABLE I. Fitting parameters used to fit Eq. (4) to experimental data presented in Fig. 5.

E (kV/cm)	A (Ω/K)	B (Ω)	T_C (K)	T_S (K)
1	0.2	3650	30	100
3	1.9	3100	25	100
6	3.1	2600	22	100
20	4.4	1700	21	100
80	4.4	1125	21	100

resistance of the conductive regions. Positive slope of dR/dT indicates that resistance of the conductive regions is determined by metallic SWCNT.

Geometrical factors A and B in Eq. (4) are determined by effective fractions of the length of the metallic regions and the insulating regions; therefore, A and B are independent of temperature. However, the fitting parameters presented in Table I demonstrate that A and B depend on electric field strength. With increasing electric field strength, factor A increases and factor B decreases, indicating that correspondingly effective length of metallic SWCNT increases and that of insulating barriers decreases. It means that in strong electric fields some of the insulating barriers are modified so that become practically transparent for electron tunneling. Thus, some of the barriers are short connected and do not contribute to the sample resistivity; therefore, effective length of the conducting regions becomes relatively larger and length of insulating barriers becomes relatively smaller. Sheng's model[13] predicts that parameter T_C in Eq. (4) is reduced by the external electric field. This corresponds to our results as presented in Table I. Dependence T_C (U) does not follow relation given in the Sheng's model probably because factors A and B are electric field-sensitive. Modification of SWCNT energy band structure by transverse electric field is predicted at much stronger electric fields (10^6–10^7 V/cm);[27] therefore, must be ruled out in our case.

It has been reported that resistivity of individual metallic SWCNT grows with electric field up to values 50 kV/cm.[17,26] This effect probably contributes to increase of factor A in Eq. (4). The increase of factor A is also related with increase of effective fraction of metallic SWCNT in SWCNT film. Similar effect was reported in SWCNT mats,[28] where the metallic term in Eq. (4) was found to depend on amount of metallic SWCNT in the SWCNT mat.

Total resistance of SWCNT film decreases with the increasing electric field within the investigated temperature range, indicating that the effect of the resistance increase in metallic SWCNT is overbalanced by the effect of increase of the barriers tunneling transparency with increasing electric field. Electrical properties of SWCNT film would approach properties on individual metallic SWCNT only in case when all the insulating barriers are shortened by strong electric field. However, this situation is hardly achievable in SWCNT films since electric fields 200 kV/cm and stronger (i.e., roughly twice as large as used in these experiments) produced permanent destruction of SWCNT films even in nanosecond time scale.

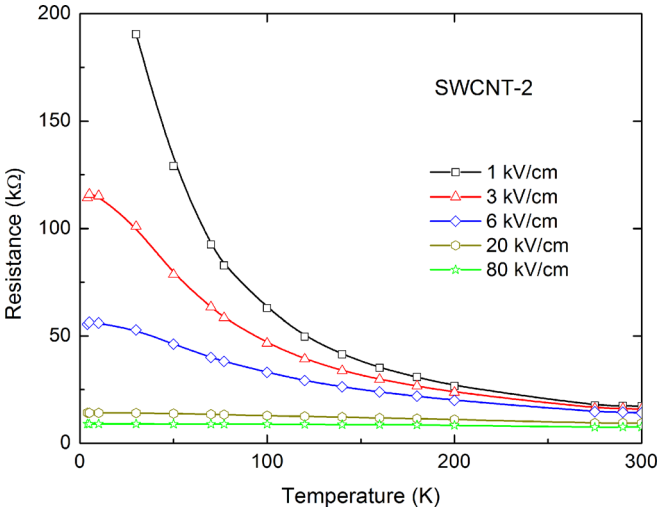

FIG. 6. Dependence of the resistance of acid-treated SWCNT layers on temperature at different electric field values. The connecting lines are for visual guidance.

In SWCNT structures, there may be combination of the homogeneously disordered part and the heterogeneous conduction part. Normally, homogeneous (VRH) model is better suitable in defective SWCNT structures; meanwhile, structures with smaller defect density follow heterogeneous (FIT) model.[29] For investigated samples, we assume co-existence of both effects. Significant contribution to conductivity from the metallic term indicates that the localization is weak.

To facilitate the localization of carriers, we prepared films of acid-treated SWCNT (sample SWCNT-2). Temperature dependences of the resistance of the acid-treated SWCNT films at various values of electric field strength are presented in Fig. 6. In acid-treated SWCNT film, the metallic conduction is no longer observed within the investigated electric field range. It is known that ultrasonication of SWCNT in acid solution reduces average length of SWCNT and produces additional defect sites.[30] We relate the absence of the metallic term in Fig. 6 with increased number of defect sites serving as localization centers. Moreover, shorter SWCNTs produce increased number of intertube contacts, which may also serve as localization centers. Significant contribution of the carrier localization and the hopping conduction mechanism is evidenced by the tendency of the resistance to diverge at temperature limit 0 K at lowest electric field value[15] (Fig. 6.).

IV. CONCLUSION

Electrical transport in SWCNT films was investigated in strong electric fields up to 10^5 V/cm in nanosecond time scale. Fitting of experimental results to the homogeneous and the heterogeneous models indicate that localization of carriers takes place in CNT films; however, tunneling through the insulating barriers between conducting regions of metallic SWCNT dominates. Crossover from semiconductor behavior to metallic behavior at electric field strength around 3 kV/cm is explained in terms of variation of transparency of the insulating barriers with the electric field strength.

ACKNOWLEDGMENTS

The authors are grateful to Professor Vilius Palenskis (Vilnius University), Professor Feodor Kusmartsev, and Professor Kirill Alekseev (Loughborough University) for valuable discussions. This research was partially supported by BRFFR (Belarus) under projects F12R-030, F12MV-004; EU FP7 under Projects FP7-318617 FAEMCAR, FP7-247007 CACOMEL and FP7-266529 BY-NanoERA.

[1]A. Bachtold, P. Hadley, T. Nakanishi, and C. Dekker, Science **294**, 1317 (2001).
[2]Y. X. Zhou, A. Gaur, S. H. Hur, C. Kocabas, M. A. Meitl, M. Shim, and J. A. Rogers, Nano Lett. **4**, 2031 (2004).
[3]Z. Wu, Z. Chen, X. Du, J. M. Logan, J. Sippel, M. Nikolou, K. Kamaras, J. R. Reynolds, D. B. Tanner, A. F. Hebard, and A. G. Rinzler, Science **305**, 1273 (2004).
[4]M. E. Itkis, F. Borondics, A. Yu, and R. C. Haddon, Science **312**, 413 (2006).
[5]R. Lu, G. Xu, and J. Z. Wu, Appl. Phys. Lett. **93**, 213101 (2008).
[6]Z. Li, P. Dharap, S. Nagarajaiah, E. V. Barrera, and J. D. Kim, Adv. Mater. **16**, 640 (2004).
[7]M. L. Terranova, M. Lucci, S. Orlanducci, E. Tamburri, V. Sessa, A. Reale, and A. Di Carlo, J. Phys. Condens. Matter **19**, 225004 (2007).
[8]N. Srivastava, H. Li, F. Kreupl, and K. Banerjee, IEEE Trans. Nanotechnol. **8**, 542 (2009).
[9]A. B. Kaiser, G. Düsberg, and S. Roth, Phys. Rev. B **57**, 1418 (1998).
[10]M. Stadermann, S. J. Papadakis, M. R. Falvo, J. Novak, E. Snow, Q. Fu, J. Liu, Y. Fridman, J. J. Boland, R. Superfine, and S. Washburn, Phys. Rev. B **69**, 201402(R) (2004).
[11]N. F. Mott and E. A. Davis, *Electronic Processes in Non-Crystalline Materials* (Clarendon, Oxford, 1979), p. 30.
[12]G. T. Kim, S. H. Jhang, J. G. Park, Y. W. Park, and S. Roth, Synth. Met. **117**, 123 (2001).
[13]P. Sheng, Phys. Rev. B **21**, 2180 (1980).
[14]M. Salvato, M. Cirillo, M. Lucci, S. Orlanducci, I. Ottaviani, M. L. Terranova, and F. Toschi, J. Phys. D: Appl. Phys. **45**, 105306 (2012).
[15]M. Salvato, M. Cirillo, M. Lucci, S. Orlanducci, I. Ottaviani, M. L. Terranova, and F. Toschi, Phys. Rev. Lett. **101**, 246804 (2008).
[16]M. S. Fuhrer, M. L. Cohen, A. Zettl, and V. Crespi, Solid State Commun. **109**(2), 105 (1998).
[17]Z. Yao, C. L. Kane, and C. Dekker, Phys. Rev. Lett. **84**, 2941 (2000).
[18]E. Pop, D. A. Mann, K. E. Goodson, and H. Dai, J. Appl. Phys. **101**, 093710 (2007).
[19]M. V. Shuba, A. G. Paddubskaya, P. P. Kuzhir, S. A. Maksimenko, V. K. Ksenevich, G. Niaura, D. Seliuta, I. Kasalynas, and G. Valusis, Nanotechnology **23**, 495714 (2012).
[20]A. F. Peterson and G. D. Durgin, *Transient Signals on Transmission Lines* (Morgan & Claypool, 2009), p. 28.
[21]L. Xiao, Z. Chen, C. Feng, L. Liu, Z.-Q. Bai, Y. Wang, Li Qian, Y. Zhang, Q. Li, K. Jiang, and S. Fan, Nano Lett. **8**, 4539 (2008).
[22]P. Liu, L. Liu, Y. Wei, K. Liu, Z. Chen, K. Jiang, Q. Li, and S. Fan, Adv. Mater. **21**, 3563 (2009).
[23]M. S. Fuhrer, W. Holmes, P. L. Richards, P. Delaney, S. G. Louie, and A. Zettl, Synth. Met. **103**, 2529 (1999).
[24]V. K. Ksenevich, V. B. Odzaev, Z. Martunas, D. Seliuta, G. Valusis, J. Galibert, A. A. Melnikov, A. D. Wieck, D. Novitski, M. E. Kozlov, and V. A. Samuilov, J. Appl. Phys. **104**, 073724 (2008).
[25]M. Jaiswal, W. Wang, K. A. S. Fernando, Y.-P. Sun, and R. Menon, J. Phys.: Cond. Matter. **19**, 446006 (2007).
[26]D. F. Santavicca, J. D. Chudow, D. E. Prober, M. S. Purewal, and P. Kim, Nano Lett. **10**, 4538 (2010).
[27]Y.-W. Son, J. Ihm, M. L. Cohen, S. G. Louie, and H. J. Choi, Phys. Rev. Lett. **95**, 216602 (2005).
[28]M. Shiraishi and M. Ata, Synth. Met. **128**, 235 (2002).
[29]R. Kamalakannan, K. Ganesan, S. Ilango, N. Thirumurugan, V. N. Singh, M. Kamruddin, B. R. Mehta, and A. K. Tyagi, Appl. Phys. Lett. **98**, 192105 (2011).
[30]M. V. Shuba, A. G. Paddubskaya, A. O. Plyushch, P. P. Kuzhir, G. Ya. Slepyan, S. A. Maksimenko, V. K. Ksenevich, P. Buka, D. Seliuta, I. Kasalynas, J. Macutkevic, G. Valusis, C. Thomsen, and A. Lakhtakia, Phys. Rev. B **85**, 165435 (2012).